

**PROGRESS REPORT FOR**

**Improved Radioimmunotherapy of  
Hematologic Malignancies**

**1988-1991**

**with emphasis on results obtained in the last funding period (1990-91)**

**DISCLAIMER**

This report was prepared as an account of work sponsored by an agency of the United States Government. Neither the United States Government nor any agency thereof, nor any of their employees, makes any warranty, express or implied, or assumes any legal liability or responsibility for the accuracy, completeness, or usefulness of any information, apparatus, product, or process disclosed, or represents that its use would not infringe privately owned rights. Reference herein to any specific commercial product, process, or service by trade name, trademark, manufacturer, or otherwise does not necessarily constitute or imply its endorsement, recommendation, or favoring by the United States Government or any agency thereof. The views and opinions of authors expressed herein do not necessarily state or reflect those of the United States Government or any agency thereof.

SUMMARY OF EXPERIMENTAL FINDINGS

Aim 1: To study the relative rates of metabolic degradation of radiolabeled monoclonal antibodies (RAbs)<sup>1</sup> targeting tumor associated antigens.

A. Survey of Endocytosis and Degradation Rates of RAbs. We have systematically studied the endocytosis, intracellular routing, and metabolism of a large panel of MoAbs recognizing the major surface antigens present on T and B lymphocytes as well as selected antibodies targeting myeloid cells, and breast cancer cells (summarized in Table I below): These experiments have documented marked variability in the rates of endocytosis and catabolism of <sup>125</sup>I-labeled MoAbs.

Table I: Characteristics of <sup>125</sup>I-Labeled MoAbs Studied

Tumor Line	MoAb (Isotype)	Endocytosis Rate*	% Degraded in 24 Hr*	Antigen Target	# Binding Sites/Cell†	Avidity (L/M)
RAMOS (B cell lymphoma)	DA4-4 (IgG1)	Fast	35-50%	IgM	330,000	4.3 x 10 <sup>9</sup>
	HD37 (IgG1)	Fast	20-30%	CD19	100,000	3.0 x 10 <sup>8</sup>
	HD6 (IgG1)	Intermediate	22%	CD22	90,000	2.9 x 10 <sup>9</sup>
	MB-1 (IgG1)	Intermediate	15%	CD37	235,000	3.0 x 10 <sup>9</sup>
	7.2 (IgG2a)	Slow	<10%	HLA DR	390,000	1.7 x 10 <sup>9</sup>
	B1 (IgG2a)	Slow	<10%	CD20	305,000	3.7 x 10 <sup>8</sup>
	BC8 (IgG1)	Slow	<10%	CD45	200,000	5 x 10 <sup>8</sup>
HPB-ALL (T cell lymphoma)	64.1 (IgG2a)	Fast	35-60%	CD3	100,000	2 x 10 <sup>9</sup>
	35.1 (IgG2a)	Fast	50%	CD2	20,000	1.5 x 10 <sup>9</sup>
	66.1 (IgG2a)	Intermediate	25%	CD4	60,000	0.7 x 10 <sup>9</sup>
	66.2 (IgG2a)	Slow	<10%	CD8	90,000	2.2 x 10 <sup>9</sup>
	BC8 (IgG1)	Slow	<10%	CD45	N.D.	N.D.
HEL (Myeloid Leukemia)	P67-6 (IgG1)	Fast	50-60%	CD33	10,000	1 x 10 <sup>10</sup>
	BC8 (IgG1)	Slow	<10%	CD45	200,000	5 x 10 <sup>8</sup>
AKR/A (Murine T Lymphoma)	OX7 (IgG1)	Slow	<10%	Thy 1.1	1,000,000	7 x 10 <sup>8</sup>
SKBR3 (Breast CA)	4D5 (IgG1)	Fast	30-55%	Her2/neu	105,000	1.6 x 10 <sup>9</sup>

\*See Figure 1 and Reference (30, 32).

†Reference (1, 2) and unpublished results.

The endocytosis and degradation rates of representative RAbs determined by cellular radioimmunoassays (see Methods and Refs 1 & 2) are depicted in Figures 1 & 2, respectively.

<sup>1</sup>Abbreviations: CT, chloramine T; HPLC, high performance liquid chromatography; MoAb, monoclonal antibody; PIB, paraiodobenzoyl; RAb, radiolabeled antibody; RIT, radioimmunotherapy; SDS-PAGE, sodium dodecyl sulfate polyacrylamide gel electrophoresis; SN, supernatant; TCA, trichloroacetic acid; TCB, tyramine cellobiose; TLC, thin layer chromatography.

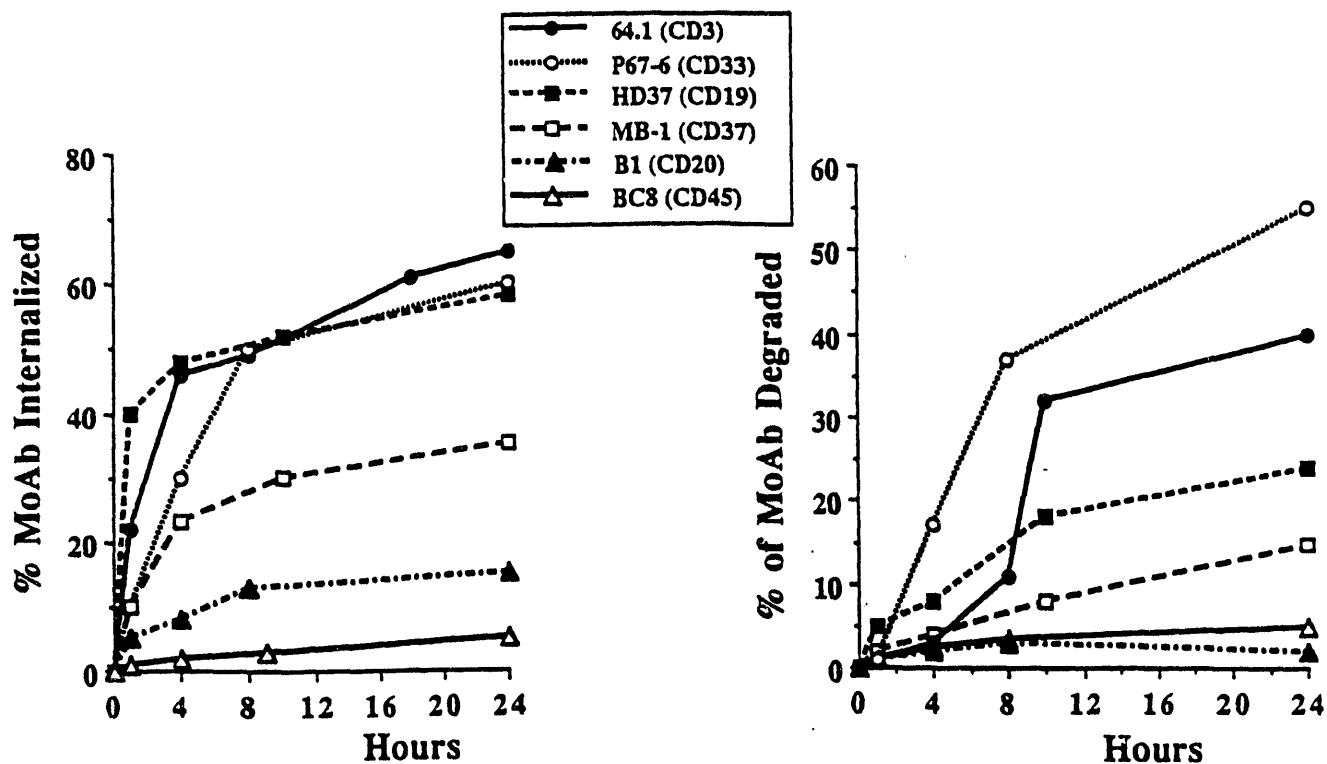


Fig. 1: Rates of Internalization of Selected RAbs by the Tumor Cell Targets listed in Table I (determined by cellular radioimmunoassay).

Fig. 2: Rates of Metabolism of RAbs by Tumor Cell Targets (determined by appearance of small molecular weight [TCA soluble]  $^{125}\text{I}$ -labeled species in culture supernatants).

B. Kinetic Analysis of RAb Internalization and Degradation. A typical kinetic profile quantifying the % of RAb present on the cell surface, inside cells, and in the culture supernatant as a function of time is shown in Fig. 3 for  $^{125}\text{I}$ -labeled anti-CD3 MoAb 64.1 targeted to the HPB-ALL T cell lymphoma line. Similar curves (albeit with different slopes) have been generated for the other MoAbs listed in Table II (1-4). In Fig. 4, the radioactivity appearing in supernatants of malignant T cells labeled with  $^{125}\text{I}$ -MoAb 64.1 is fractionated into small molecular weight species (<10,000 kD) which are soluble in 25% trichloroacetic acid (TCA), and large molecular weight species which are TCA-precipitable. It can be seen that early in the culture period (<4 hours), most of the supernatant radioactivity is TCA precipitable (primarily intact RAbs passively dissociated from cell surface antigenic sites), whereas late in the culture period, the majority of radioactivity released from cells is present as small molecular weight species (characterized by SDS-PAGE, HPLC, and TLC in Aim 3 below).

Recent studies in our laboratory have shown that antibody internalization and degradation are identical for MoAbs radioiodinated using the IodoGen technique or biosynthetically labeled by incubation of hybridoma cells with  $^3\text{H}$ -leucine. These data show that the patterns of cellular internalization and degradation for the radioiodinated antibodies faithfully mimic those of native antibody and are not due to protein damage during the iodination process as can occur when harsher iodination conditions are used (5).

C. Morphologic documentation of intracellular routing. Immunoperoxidase electron microscopy and ultrastructural autoradiography have been used to directly observe the trafficking of antibody conjugates from the cell surface through clathrin-coated pits to endosomes and lysosomes (1,2, 6). (See Appendix I Figures 1-3 for photomicrographs).

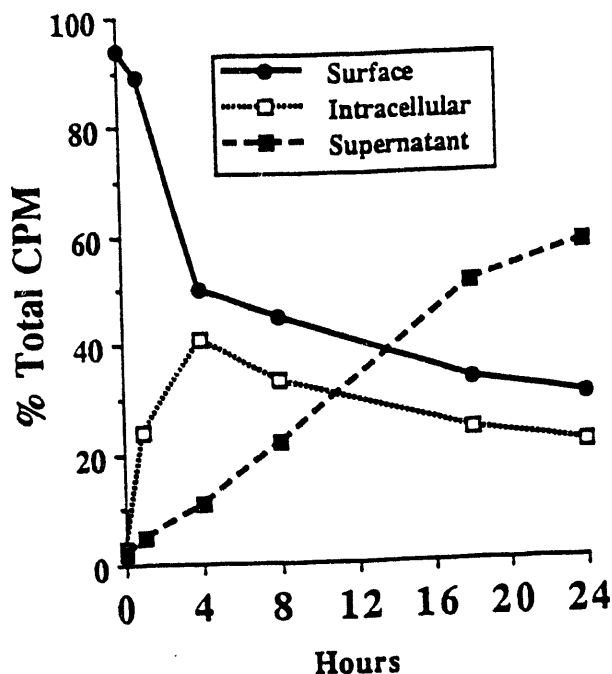


Fig. 3: Distribution of  $^{125}\text{I}$ -MoAb 64.1 on the Cell Surface, Intracellularly, and in Culture Supernatants as a Function of Time after Targeting HPB-ALL cells (determined by cellular radioimmunoassay).

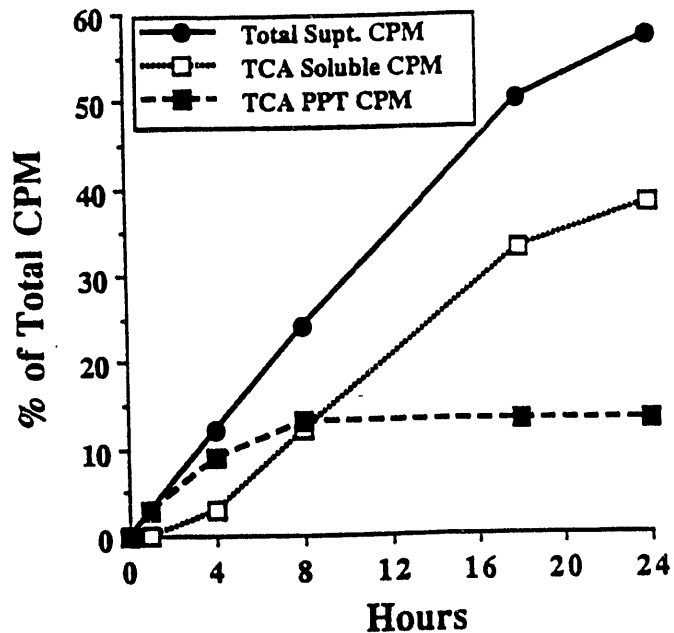


Fig. 4: Accumulation of TCA-soluble, TCA-precipitable, and total cpm in culture supernatants of HPB-ALL cells pulse-labeled at time 0 with  $^{125}\text{I}$ -MoAb 64.1.

*Aim 2: To examine the effects of lysosomotropic amines ( $\text{NH}_4\text{Cl}$ , chloroquine, amantadine), carboxylic ionophores (monensin, nigericin), and thioamides (propylthiouracil), on the retention of radiolabeled MoAbs by tumor cells.*

A. In vitro Assessment of Pharmacologic Agents on RAb Metabolism. A variety of pharmacologic agents (listed above) have been shown to interfere with catabolism of  $^{125}\text{I}$ -labeled protein ligands (3,7-13). We have tested the hypothesis that these agents can be used to retard degradation of radioimmunoconjugates by tumor cells and augment the retention of RAbs by tumors. The success of this approach *in vitro* is documented in Figs 5 & 6 which demonstrate that the tested drugs decrease the degradation of  $^{125}\text{I}$ -64.1 by T lymphoma cells by 15-90% at nontoxic doses (Fig.5) and augment retention of the RAb by 150-330% at 24 hours of culture (Fig. 6)

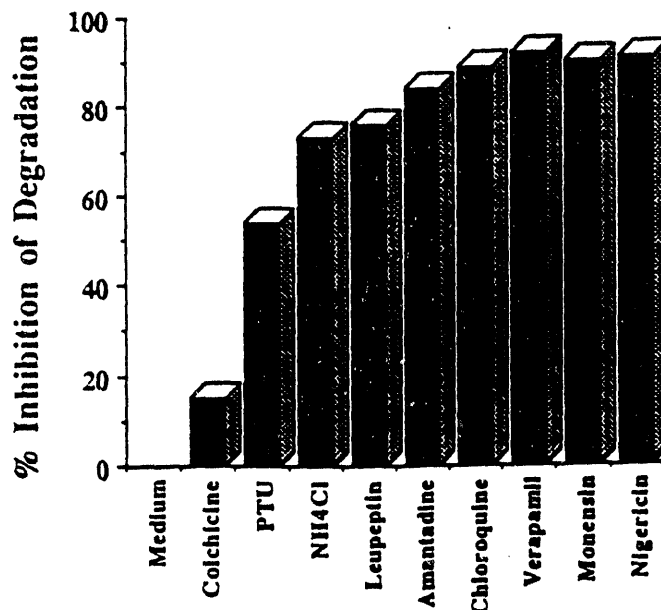


Fig. 5: Inhibition of  $^{125}\text{I}$ -MoAb 64.1 Degradation by HPB-ALL cells by 20  $\mu\text{M}$  colchicine, 10 mM propylthiouracil, 20 mM NH<sub>4</sub>Cl, 400  $\mu\text{M}$  leupeptin, 2.5 mM amantadine, 0.8 mM chloroquine, 0.64 mM verapamil, 10  $\mu\text{M}$  monensin, and 10  $\mu\text{M}$  nigericin (as determined by appearance of TCA soluble cpm in culture supernatants).

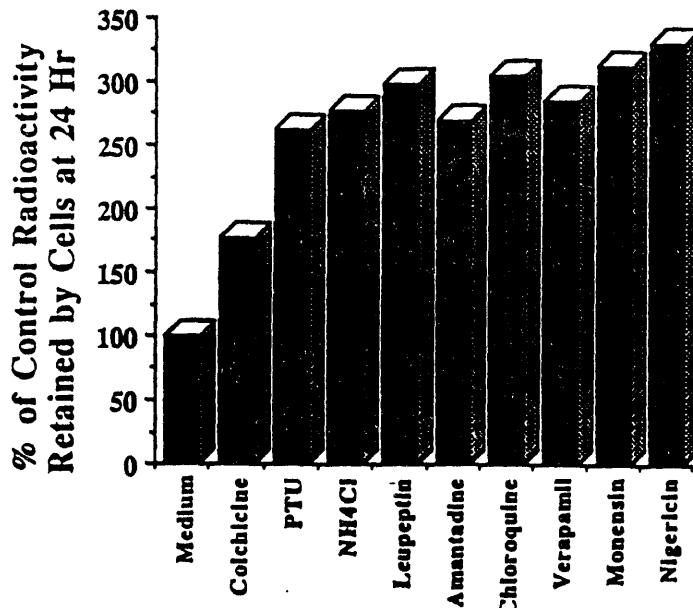


Fig. 6: Augmented Retention of  $^{125}\text{I}$ -MoAb 64.1 by HPB-ALL cells after 24 hours of culture with the pharmacologic agents listed in Fig. 5.

**B. Assessment of Toxicity of Pharmacologic Agents *in vivo*.** Although the pharmacologic agents investigated work dramatically *in vitro* (Figs. 5 & 6), their effective clinical implementation depends upon whether they can be administered at effective concentrations *in vivo* with tolerable toxicity. To determine the maximally tolerated doses of these drugs in a murine model, escalating concentrations were administered to groups of BALB/c mice (5 each) as outlined in the original application. Table II summarizes the highest doses of drugs which could be administered without observing *any* toxic deaths.

Table II: Maximally Tolerated Doses of Lysosomotropic Agents

Drug	Maximally Tolerated Dose
<i>Single Agents</i>	
Monensin	6 mg/kg IP twice daily for 5 days
Chloroquine	70 mg/kg IP twice daily for 5 days
Verapamil	25 mg/kg IP twice daily for 5 days
Propylthiouracil	100 mg/kg IP daily for 7 days
Amantadine	100 mg/kg IP daily for 7 days
Leupeptin	>40 mg/kg IP daily for 7 days

*by Osmotic Pump*

	<i>by continuous subcutaneous infusion</i>
Monensin	not feasible--precipitates in pump
Chloroquine	320 mg/kg subQ for 7 days
Verapamil	72 mg/kg sub Q for 7 days

*Combinations*

	<i>by Intraperitoneal Injection</i>
Monensin + Chloroquine	6 mg/kg + 20 mg/kg IP twice daily for 2 days
Monensin + Verapamil	6 mg/kg + 12 mg/kg IP twice daily for 2 days

Aim 3: To identify the subcellular site of radioimmunoconjugate degradation, and to quantify the sizes of the fragments generated by intracellular metabolism of radiolabeled antibodies.

A. Analysis of trafficking through subcellular compartments. Percoll density gradient sedimentation of organelles was used to analyze the intracellular routing of RAbs in tumor cells which had been pulse-labeled with RAbs and then disrupted with a Dounce homogenizer. With this technique, buoyant surface membrane and endosomal fractions (sp. grav. 1.010-1.035) were easily separated from the dense lysosomal fraction (sp. grav. 1.080). The position of organelles on these gradients was documented by marker enzyme analyses (5' nucleotidase and alkaline phosphodiesterase for plasma membrane;  $\beta$  galactosidase for lysosomes) and by electron microscopy (see Appendix I, Figure 4). A typical experiment is shown in Figs. 7 & 8 for HPB-ALL cells pulse-labeled with  $^{125}\text{I}$ -MoAb 64.1. At time 0, virtually all  $^{125}\text{I}$ -64.1 was on the cell surface whereas by 8 hours the majority was present in lysosomes, and by 24 hours all radioactivity had been cleared from the cell surface and the total amount of cell associated radioactivity ("area under the curve") was markedly diminished, presumably due to lysosomal degradation and exocytosis of RAbs.

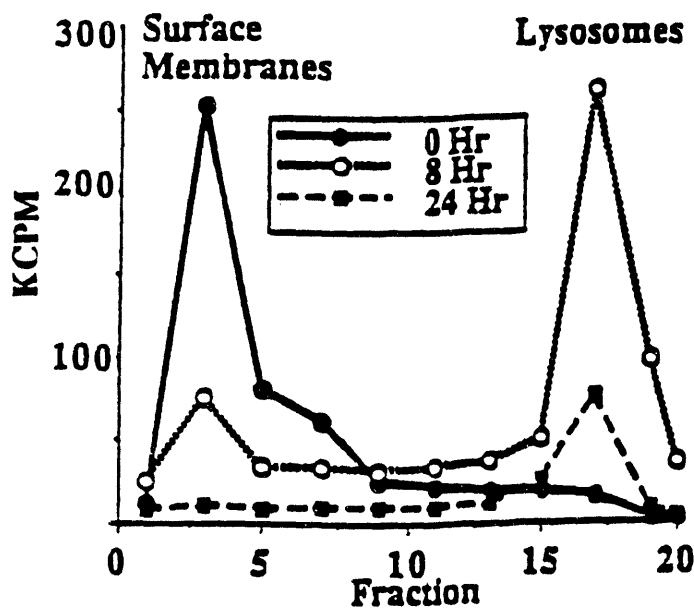


Fig. 7: Transit of  $^{125}\text{I}$ -MoAb 64.1 from buoyant (cell surface/endosomal) fractions to dense (lysosomal) fractions on 20% Percoll gradients as a function of time (using HPB-ALL cells).

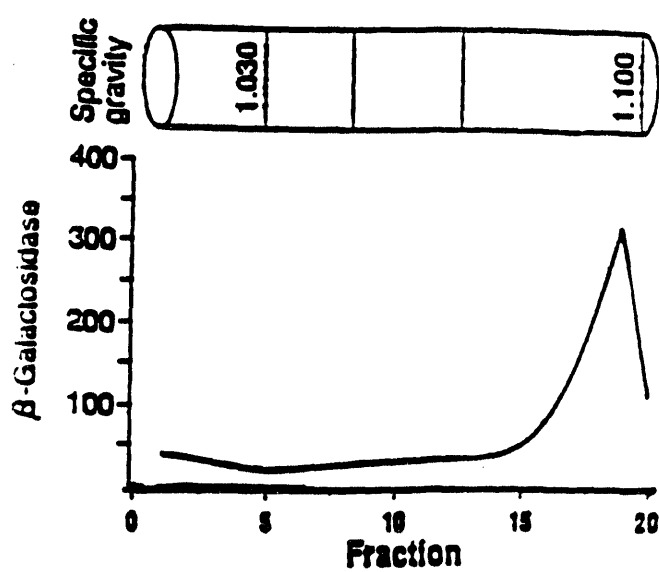


Fig. 8: Distribution of the lysosomal enzyme  $\beta$ -galactosidase on the same 20% Percoll gradient depicted in Figure 7.

B. Biochemical analysis of metabolites. Target cells incubated for various periods of time at 37°C with  $^{125}\text{I}$ -labeled RAbs were lysed and analysed by HPLC, SDS-PAGE, and thin layer chromatography (TLC) to determine the sizes of generated fragments. The tempo of RAb degradation was monitored for whole cell lysates, for lysates of organelles purified on Percoll gradients, and for culture supernatants at time intervals ranging from 1-24 hours after pulse-labeling target cells with RAbs. A typical experiment using  $^{125}\text{I}$ -MoAb DA4-4 targeted to RAMOS

cells is depicted in the SDS-PAGE and TLC autoradiographs in Appendix I, Figs. 5a & 5b. This experiment shows progressive accumulation of intermediate-sized RAb metabolites (50 kD, 28 kD, 25 kD, and 12 kD) inside B lymphoma cells beginning 4 hours after tumor cell targeting. Studies using organelle fractions demonstrated a minimal amount of RAb metabolism in prelysosomal endosomes, with >95% of degradation occurring in the lysosomal fraction (data not shown). Analysis of culture supernatants revealed that these intermediate sized fragments were not exocytosed from tumor cells in detectable quantities (data not shown), and that >95% of TCA-soluble supernatant radioactivity (>70% of *total* supernatant radioactivity) was present as  $^{125}\text{I}$ -tyrosine. Contrary to popular belief, free  $^{125}\text{I}$  represented <10% of culture radioactivity. These results suggest that the process of "dehalogenation" reported by most authors in fact consists primarily of terminal degradation of RAbs to  $^{125}\text{I}$ -tyrosine by lysosomal hydrolases rather than liberation of free  $^{125}\text{I}$  from RAbs by "deiodinases". This distinction can not be made using TCA precipitation, standard SDS-PAGE or size-exclusion HPLC; thin layer chromatography (as employed here) or reverse phase HPLC is required.

**C. Effect of pharmacologic agents on RAb Metabolism in Lysosomes.** Tumor cells pulse-labeled with  $^{125}\text{I}$ -RAbs and cultured for 18 hours at 37°C in the absence or presence of optimal concentrations of lysosomotropic agents were disrupted with a Dounce apparatus, sedimented on 20% Percoll gradients, and analyzed by gamma counting organelle fractions to assess the impact of these drugs on lysosomal degradation of RAbs. As shown in Fig. 9, all the agents markedly enhanced the retention of radioactivity in the lysosomal fraction of tumor cells. Analysis of cell lysates by SDS-PAGE (not shown) and by TLC (Appendix I, Fig. 5b) showed that the sizes of metabolic fragments generated were not altered by the pharmacologic agents, but that the amount of degradation occurring in a given time period was markedly diminished.

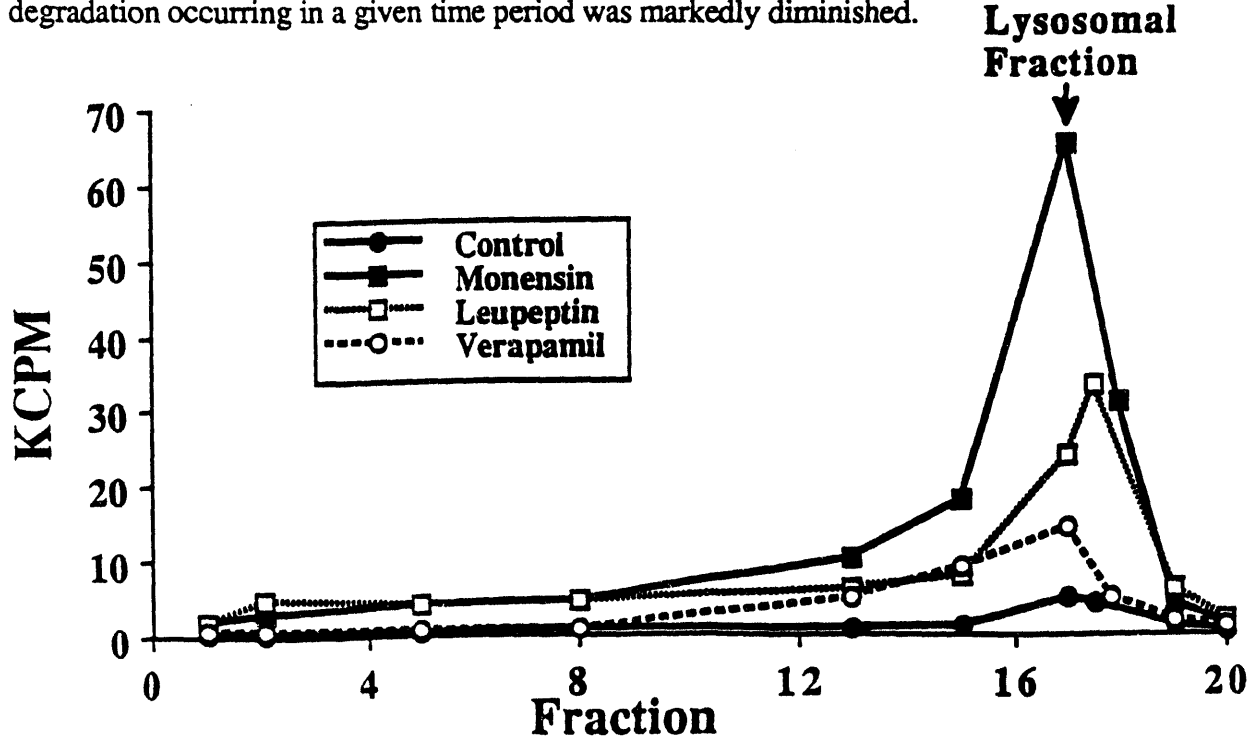


Fig. 9: Effect of pharmacologic agents on the retention of  $^{125}\text{I}$ -MoAb DA4-4 by lysosomes in RAMOS cells 18 hours after pulse-labeling with 1  $\mu\text{M}$  monensin, 200  $\mu\text{M}$  leupeptin, 200  $\mu\text{g/ml}$  verapamil, or no agent (control).

**Aims 4 & 5: To examine the effects of lysosomotropic agents on radioimmuno-scintigraphy and radioimmunotherapy.**

**A. Effect of pharmacologic agents on Biodistribution of RAbs in Beige/Nude Mice Bearing Tumor Xenografts.** We administered 150  $\mu\text{g}$  monensin subcutaneously every 12 hours for 2 days to

nude/beige mice (groups of 5 each) bearing 0.5-1.0 cm diameter Her2/neu tumor xenografts beginning 12 hours before injection of 10  $\mu$ g/25  $\mu$ Ci  $^{131}$ I-labeled MoAb 4D5 (anti-Her2/neu) and an  $^{125}$ I-labeled, isotype-matched control MoAb. Mice were euthanized 48 & 96 hours after RAb injection and the biodistributions of relevant and irrelevant RAbs in tumor, blood, and normal organs measured by gamma counting (after correcting for radioactive decay and crossover of  $^{131}$ I into the  $^{125}$ I channel). In these pilot experiments, a modest (25%) improvement in tumor retention was observed (see Fig. 10). Although this finding is encouraging, it is less impressive than we had anticipated from our *in vitro* experiments. We suspect that the limited aqueous solubility of monensin and its rapid serum clearance (14, 15) may have mitigated the beneficial effects of this ionophore *in vivo*. Two approaches are being investigated to improve the bioavailability of this potentiating agent. First, monensin-albumin conjugates are being synthesized since they have been shown to have a prolonged serum half-life and a greater *in vivo* potentiating effect for ricin A chain immunotoxins compared with unmodified monensin (16, 17). Secondly, liposomal monensin is being investigated since it has been shown to be 500-fold more potent than unmodified monensin ([15] see below). Further experiments will be necessary to ascertain whether other agents or combinations of agents (see Table II) will yield superior results, and whether this approach will ultimately result in improved radioimmunoscintigraphy and radioimmunotherapy.

B. Novel new formulation of carboxylic ionophores. Dr. Thomas Griffin and Dr. Ali Salimi at the University of Massachusetts (Worcester) have recently described the preparation of liposomal monensin (15). This formulation represents a major advance over the aqueous and lipid emulsion formulations which we and others have been using with monensin, since it assures sustained systemic concentrations of this lipophilic drug, and has been shown to be 500-fold more efficacious than aqueous monensin in potentiating the efficacy of ricin A-chain immunotoxins *in vivo* (15). Whether this will be true for RAbs as well as immunotoxins remains to be tested, though our recent studies with liposomal monensin *in vitro* indicate a marked potency advantage over conventional monensin formulations (Fig. 11).

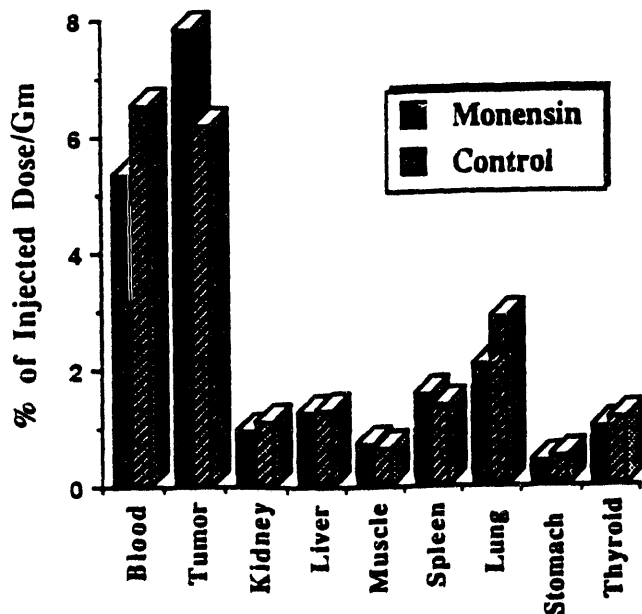


Fig. 10: Biodistribution of  $^{125}$ I-MoAb 4D5 in Her2/neu tumor xenografts and in normal organs 48 hours after injection in the presence and absence of unmodified monensin (150  $\mu$ g subcutaneously q 12 hours x 4 doses).

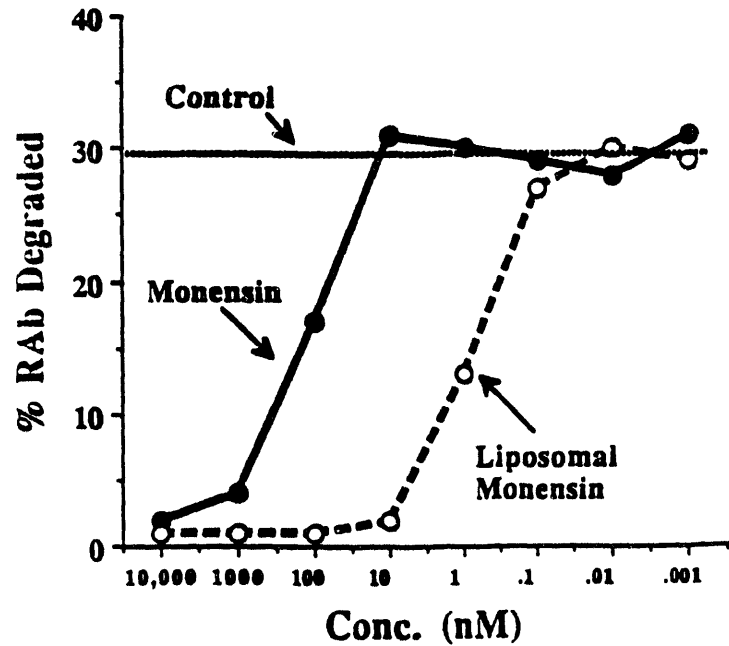


Fig. 11: Superiority of liposomal monensin compared with unmodified monensin in augmenting the retention of  $^{125}$ I-MoAb DA4-4 by RAMOS cells *in vitro*. Note the logarithmic scale.

Aim 6: To compare the patterns of metabolic degradation of radioimmunoconjugates made with different conjugation techniques and with different radionuclides. We have recently shown that novel, new radioiodination techniques using nonmetabolizable aryl carbohydrate adducts (e.g. tyramine cellobiose, tyramine glucose) to link  $^{131}\text{I}$  to MoAbs result in prolonged trapping of polar TCB- $^{131}\text{I}$  metabolites inside lymphoma cells (46). We have recently confirmed these findings using the anti-CD33 MoAb P67-6, which is used clinically at our institution to target  $^{131}\text{I}$  to acute myeloid leukemia cells (Fig. 12 & 13). Conventional  $^{125}\text{I}$ - or  $^{131}\text{I}$ -labeled P67-6 RAbs made using the chloramine T or IodoGen methods are rapidly internalized and degraded by leukemia cells, with resultant rapid release of small molecular weight, TCA-soluble metabolites (Fig. 12). In contrast,  $^{131}\text{I}$ -TCB-P67-6 constructs are degraded one third as rapidly (Fig. 12) and the amount of cell associated radioactivity after 24 hours of culture is doubled using this novel new method (Fig. 13).

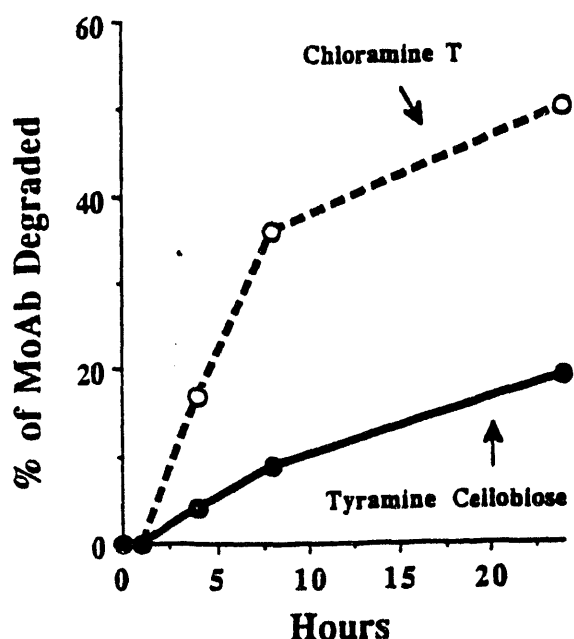


Fig. 12: Diminished rate of degradation of  $^{125}\text{I}$ -MoAb P67-6 by HEL cells after conjugation by the tyramine cellobiose method compared with the chloramine T method (as determined by rate of accumulation of TCA soluble cpm in culture supernatants).

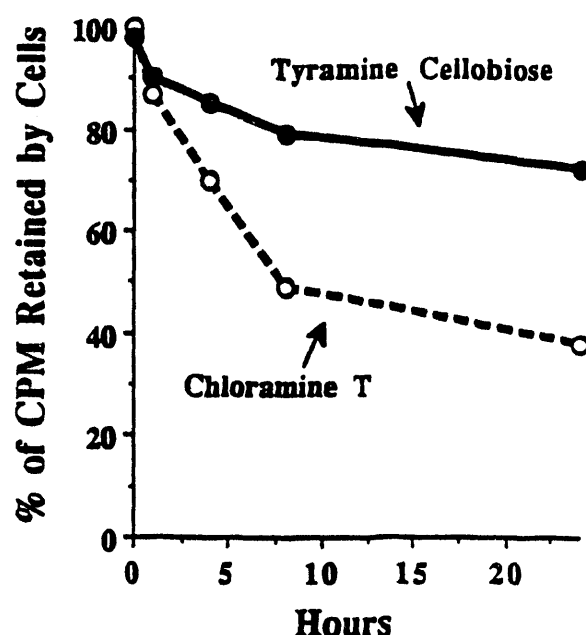


Fig. 13: Enhanced retention of  $^{125}\text{I}$ -MoAb P67-6 by HEL cells after conjugation by the tyramine cellobiose method compared with the chloramine T method.

Time has not yet permitted comparative analyses of metabolism of RAbs made with radiometals ( $^{111}\text{Indium}$ ,  $^{90}\text{Yttrium}$ ,  $^{99\text{m}}\text{Technetium}$ ,  $^{186}\text{Rhenium}$ ), though these experiments are planned in conjunction with our collaborators in the Division of Nuclear Medicine (Drs. Nelp and Venkatesan).

**Preliminary Results For Her2Neu Project (Aim 5 in the renewal application; not described in original application).**

As mentioned in the Background section of this grant we have been investigating the potential utility of targeting the p185 Her2/neu oncoprotein expressed on the surface membrane of poor prognosis breast and ovarian cancer patients in collaboration with Dr. Dennis Slamon (UCLA).

Initial cellular radioimmunoassays have documented the pattern of endocytosis and degradation of the 4D5 MoAb targeting this molecule (Fig. 14). Experiments in a beige/nude mouse xenograft system have documented the specific localization of injected  $^{131}\text{I}$ -4D5 to Her2/neu bearing tumors (Fig. 15). Tumor to non-tumor ratios of 5-10 to 1 were observed (Fig. 16). Pilot studies have documented the radioimmunotherapeutic efficacy of this approach (Fig. 17), though all tumors have eventually regrown at the three dose schedules tried so far. Further animal experimentation is required in this exciting new system before its application to refractory human breast cancers can be contemplated.

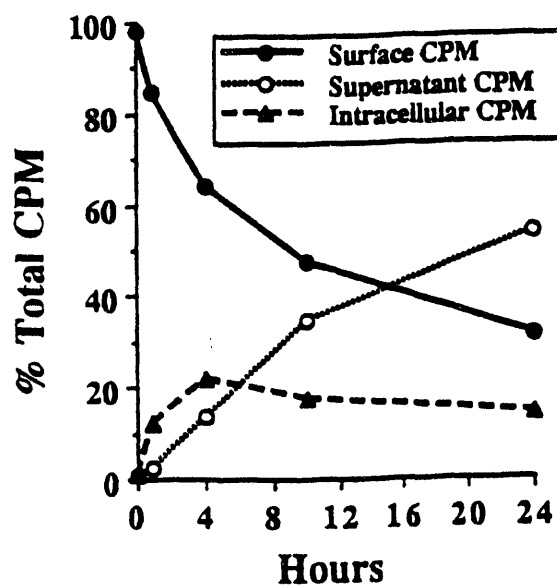


Fig. 14: Distribution of  $^{125}\text{I}$ -MoAb 4D5 on the surface, intracellularly, and in the supernatant of Her2/neu-transfected NIH3T3 cells as a function of time after pulse-labeling.

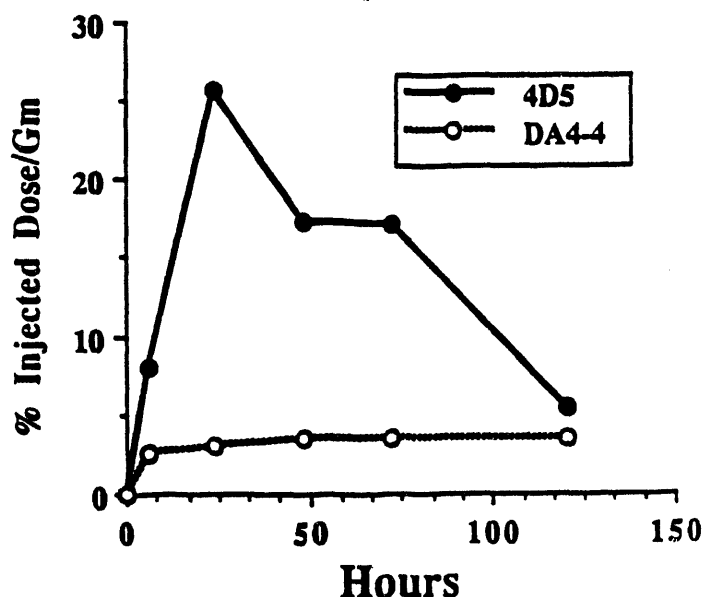


Fig. 15: Localization of  $^{131}\text{I}$ -labeled anti-Her2 neu MoAb 4D5 (10  $\mu\text{Ci}/10 \mu\text{g}$ ) and  $^{125}\text{I}$ -labeled control MoAb DA4-4 to Her2/neu expressing tumor xenografts in nude mice (expressed as % of the injected dose/gram of tumor).

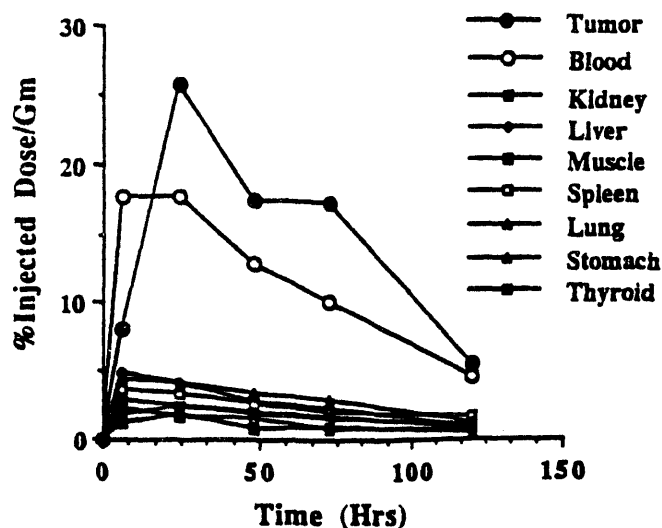


Fig.16: Biodistribution of  $^{131}\text{I}$ -labeled anti-Her2/neu MoAb 4D5 (10  $\mu\text{Ci}/10 \mu\text{g}$ ) in tumor and normal organs as a function of time.

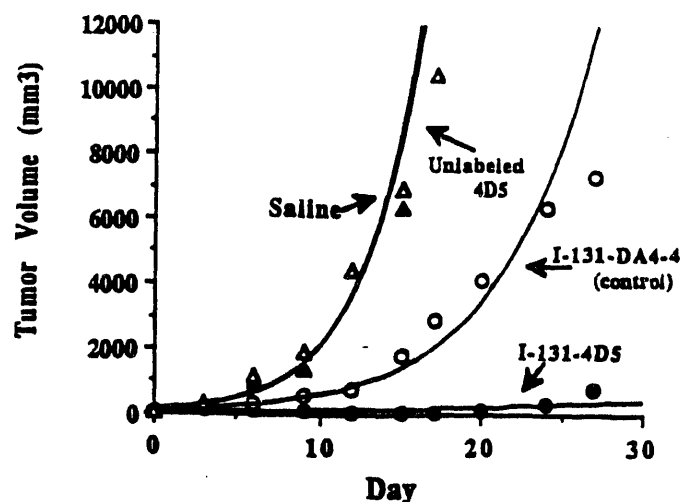


Fig. 17: Inhibition of growth of Her2/neu expressing tumor xenografts in beige/nude mice injected on Day 0 with a single dose of anti-Her2/neu RAb  $^{131}\text{I}$ -4D5 (400  $\mu\text{Ci}/45 \mu\text{g}$ ),  $^{131}\text{I}$ -DA4-4 (400  $\mu\text{Ci}/45 \mu\text{g}$  of nonbinding MoAb), 45  $\mu\text{g}$  unradiolabeled MoAb 4D5, or saline.

**Publications Resulting from DOE grant DE-FG06-88ER60719 between 1988-91:**

1. Press OW, Hansen JA, Farr A, and Martin PJ. Endocytosis and degradation of murine anti-human CD3 monoclonal antibodies. *Cancer Research* 48: 2249-2257, 1988.
2. Press OW, Eary J, Badger C, Appelbaum FA, Martin PJ, Levy R, Miller R, Brown S, Nelp WB, Krohn KA, Fisher D, DeSantes K, Porter B, Kidd P, Thomas ED, and Bernstein ID. Treatment of patients with refractory non-Hodgkin's lymphomas with radiolabeled MB-1 (anti-CD37) antibody. *Journal of Clinical Oncology* 7: 1027-1038, 1989.
3. Press OW, Farr A, Borroz I, Anderson S, and Martin PJ. Endocytosis and degradation of monoclonal antibodies targeting human B cell malignancies. *Cancer Research* 49: 4906-4912, 1989.
4. Press OW, Eary J, Badger C, Martin PJ, Appelbaum FA, Nelp WB, Krohn KA, Fisher D, Porter B, Thomas ED, Miller R, Brown S, Levy R, and Bernstein ID. High dose radioimmunotherapy of B cell lymphomas. In *Frontiers in Radiation Therapy and Oncology*, Vol. 24. (J. Vaeth, ed.) , S. Karger AG, Basel, pp. 204-213, 1989.
5. Press OW, Martin PJ, Thorpe PE, and Vitetta ES. Immunotoxins directed against different epitopes on the CD2 molecule differ in their ability to kill normal and malignant T cells. *J. Immunol.* 141: 4410-4417, 1988.

6. Ali SA, Warren SD, Richter KY, Badger CC, Eary JF, Press OW, Krohn KA, Bernstein ID, and Nelp WB. Improving the tumor retention of radioiodinated antibody: aryl carbohydrate adducts. *Cancer Research* (Suppl.) 50: 783s-788s, 1990.
7. Press OW, DeSantes KD, Anderson SK, and Geissler F. Inhibition of catabolism of radiolabeled antibodies by tumor cells using lysosomotropic amines and carboxylic ionophores. *Cancer Research* 50: 1243-1250, 1990.
8. Press OW, Eary J, Badger CC, Martin PJ, Appelbaum FA, Levy R, Miller R, Nelp WB, Krohn KA, Fisher D, Matthews D, and Bernstein ID. Radiolabeled antibody therapy of human B cell lymphomas. In *Advances in Experimental Biology and Medicine "Immunobiology of Proteins and Peptides VI"* (M.Z. Atassi, ed.), Plenum Press, New York. (In press, 1991).

Manuscripts Submitted:

9. Van der Jagt R, Appelbaum F, Eary J, Press O, Bernstein I, and Badger C. Radioimmunotherapy of myeloid leukemia with an  $^{131}\text{I}$ -labeled anti-CD33 antibody (submitted, 1991).
10. Geissler F, Anderson SK, and Press O. Intracellular catabolism of radiolabeled anti-CD3 antibodies by leukemic T cells (submitted, 1991).
11. DeSantes K, Slamon D, Press O. Targeting the Her2/Neu oncoprotein for radioimmunotherapy of cancer (submitted, 1991).
12. Hui TE, Fisher DR, Press O, Weinstein J, Badger C, and Bernstein I. Localized beta dosimetry of  $^{131}\text{I}$ -labeled antibodies in follicular lymphoma (submitted, 1991).
13. Venkatesan P, Eary J, Krohn K, Press O, Badger C, Bernstein I, and Nelp W. Enhanced retention of tyramine cellobiose radioimmunoconjugates by tumor cells. (in preparation, 1991).

Abstracts:

1. Press OW, Eary J, Badger C, Martin PJ, Appelbaum FA, Nelp WB, Krohn KA, Fisher D, Porter B, Thomas ED, Miller R, Brown S, Levy R, and Bernstein ID. "High dose radioimmunotherapy of NonHodgkin's Lymphomas", Proc. San Francisco Cancer Symposium, February, 1989.
2. Press OW, Eary J, Badger C, Martin PJ, Appelbaum FA, Nelp WB, Krohn KA, Fisher D, Porter B, Thomas ED, Miller R, Brown S, Levy R, and Bernstein ID. "Radioimmunotherapy of refractory human malignant B cell lymphomas". Proc. Am. Soc. Clin. Onc. May, 1989.
3. Press OW, De Santes K, Anderson SK, and Geissler F. Inhibition of catabolism of radiolabeled antibodies by tumor cells using lysosomotropic amines and carboxylic ionophores. *Antibody Immunoconjugates and Radiopharmaceuticals* 3: p. 48, 1990.
4. DeSantes K, Ulrich A, Langton B, Slamon D, and Press OW. Radiolabeled antibody targeting of the HER-2/neu oncoprotein. *Proc. Am. Assoc. for Cancer Res.* 31: p. 287, 1990.
5. Geissler F and Press OW. Endocytosis and degradation of radiolabeled anti-CD3 antibodies by malignant human T cells. *Proc. Am. Assoc. for Cancer Res.* 31: p. 291, 1990.

Presentations at National Meetings Concerning Research from this Grant:

1. 24th Annual San Francisco Cancer Symposium, (Invited Plenary Speaker, February 10-11, 1989).
2. American Society of Clinical Oncology, San Francisco, (Slide Presentation, May 21-23, 1989).
3. 5th International Conference on Monoclonal Antibody Immunoconjugates for Cancer, (San Diego, Slide and poster presentations, March 15-17, 1990).

4. 81st meeting of the American Association for Cancer Research, Washington D.C., (Poster presentation, May 23-26, 1990).
5. M.D. Anderson Cancer Center, Houston, TX, (Invited Speaker, October 17, 1990).
6. 6th International Symposium on Immunobiology of Proteins and Peptides, Scottsdale, AZ, (Invited Plenary Speaker, October 26-30, 1990).
7. Keystone Symposium on Monoclonal Antibodies, Denver, Colorado, (Invited Plenary Speaker, March 10-16, 1991).
8. 33rd Annual American Cancer Society Science Writers Convention, (Invited Speaker, March 24-26, 1991).

**Graduate Students Trained by this Grant:**

Dr. Francis Geissler

Thesis: Internalization and Degradation of Radioimmunoconjugates by malignant human lymphoid cells. (Ph.D. awarded: December, 1990.)

**Post-doctoral Fellows Trained by this Grant:**

Dr. Kenneth DeSantes

Project: Radiolabeled antibody targeting of the HER-2/neu oncoprotein (1988-present).

**LITERATURE CITED**

1. Press OW, Farr AG, Borroz KI, Anderson SK, and Martin PJ, Cancer Research 49: 4906-4912, 1989.
2. Press OW, Hansen JA, Farr A, and Martin PJ, Cancer Research 48: 2249-2257, 1988.
3. Press OW, DeSantes K, Anderson SK, and Geissler F, Cancer Research 50: 1243-1250, 1990.
4. Press OW, Martin PJ, Thorpe PE, and Vitetta ES, J. Immunol. 141: 4410-4417, 1988.
5. Opresko L, Wiley HS, and Wallace RA, Proc. Natl. Acad. Sci. USA 77: 1556-1560, 1980.
6. Geissler F, Anderson SK, and Press OW, "Intracellular catabolism of radiolabeled anti-CD3 antibodies by leukemic T cells" (submitted 1991).
7. Wibo M and Poole B, J. Cell Biol. 63: 430-440, 1974.
8. Pohlmann R, Kruger S, Hasilik A, and Von Figura K, Biochem. J. 217: 649-658, 1984.
9. Wileman F, Boshans RL, Schlesinger P, and Stahl P, Biochem. J. 220: 665-675, 1984.
10. Tartakoff AM, Cell 32: 1026-1028, 1983.
11. Ohkuma S and Poole B, Proc. Natl. Acad. Sci. USA 75: 3327-3331, 1978.
12. Casellas P and Jansen FK, in Immunotoxins, (Frankel AE, ed.), Kluwer Academic Publishers, pp. 351-369, 1988.
13. Tolleshaug H and Berg T, Exp. Cell Research 134: 207-217, 1981.
14. Griffin TW, Richardson C, Houston LL, LePage D, Bogden A, and Raso V, Cancer Research 47: 4266-4270, 1987.
15. Griffin T, Rybak ME, Recht L, Raso V, and Salimi A, "Liposomal monensin (Lipo Mon) for the 'in vitro' potentiation of anti-tumor immunotoxins", Proc. Second Int. Symposium on Immunotoxins, Lake Buena Vista, Florida, June 14-16, 1990.
16. Colombatti M, Dell'Arciprete L, Chignola R, and Tridente G, Cancer Research 50: 1385-1391, 1990.
17. Hertler AA, Schlossman DM, Borowitz MJ, Blythman HE, Casellas P, and Frankel AE, Int. J. Cancer 43: 215-219, 1989.



DATE  
FILED  
APR 12 1994

